JOURNAL OF GEOPHYSICAL RESEARCH, VOL. 114, D00F09, doi:10.1029/2008JD011337, 2009

Impacts of background ozone production on Houston and Dallas, Texas, air quality during the Second Texas Air Quality Study field mission

R. Bradley Pierce,[1] Jassim Al-Saadi,[2] Chieko Kittaka,[3] Todd Schaack,[4] Allen Lenzen,[4] Kevin Bowman,[5] Jim Szykman,[6] Amber Soja,[7] Tom Ryerson,[8] Anne M. Thompson,[9] Pawan Bhartia,[10] and Gary A. Morris[11]

Received 21 October 2008; revised 19 February 2009; accepted 6 March 2009; published 23 May 2009.

[1] A major objective of the 2006 Second Texas Air Quality Study (TexAQS II) focused on understanding the effects of regional processes on Houston and Dallas ozone nonattainment areas. Here we quantify the contributions of background (continental scale) ozone production on Houston and Dallas air quality during TexAQS II using ensemble Lagrangian trajectories to identify remote source regions that impact Houston and Dallas background ozone distributions. Global-scale chemical analyses, constrained with composition measurements from instruments on the NASA Aura satellite, are used to provide estimates of background composition along ensemble back trajectories. Lagrangian averaged O_3 net photochemical production (production minus loss, P-L) rates along the back trajectories are used as a metric to classify back trajectories. Results show that the majority (6 out of 9 or 66%) of the periods of high ozone in Houston were associated with periods of enhanced background ozone production. Slightly less than 50% (7 out of 15) of the days with high ozone in the Dallas Metropolitan Statistical Area (MSA) show enhanced background ozone production. Source apportionment studies show that 5-day Lagrangian averaged O_3 P-L in excess of 15 ppbv/d can occur during continental-scale transport to Houston owing to NO_y enhancements from emissions within the Southern Great Lakes as well as recirculation of the Houston emissions. Dallas background O_3 P-L is associated with NO_y enhancements from emissions within Chicago and Houston.

Citation: Pierce, R. B., et al. (2009), Impacts of background ozone production on Houston and Dallas, Texas, air quality during the Second Texas Air Quality Study field mission, *J. Geophys. Res.*, *114*, D00F09, doi:10.1029/2008JD011337.

1. Introduction

[2] The Texas Air Quality Study (TexAQS) focused on understanding the meteorological and chemical processes that lead to high-pollution events within east Texas. The major thrust of the 2000 TexAQS study was characterizing the effects of local emissions and meteorology on ozone pollution in the Houston-Galveston-Brazoria (HGB) area [*Berkowitz et al.*, 2004; *Daum et al.*, 2004; *Ryerson et al.*, 2003]. The Second Texas Air Quality Study (TexAQS II) in 2006 focused on understanding the meteorological and chemical processes that lead to high-pollution events within both the HGB and Dallas−Fort Worth (DFW) ozone nonattainment areas, with a strong emphasis on regional processes. The TexAQS field studies supported the Texas Commission on Environmental Quality (TCEQ) in developing State Implementation Plans (SIPs) for attaining National Ambient Air Quality Standards (NAAQS) for ozone in the HGB and DFW ozone nonattainment areas. Regional science questions that received special emphasis during TexAQS II included: (1) How do emissions from local and distant sources interact to determine the air quality in Texas? (2) What meteorological and chemical conditions

[1]Center for Satellite Applications and Research, Cooperative Research Program, Advanced Satellite Products Branch, NESDIS, NOAA, Madison, Wisconsin, USA.
[2]Chemistry and Dynamics Branch, Science Directorate, NASA Langley Research Center, Hampton, Virginia, USA.
[3]Science Systems and Applications, Inc., Hampton, Virginia, USA.
[4]Space Science and Engineering Center, University of Wisconsin, Madison, Wisconsin, USA.
[5]Jet Propulsion Laboratory, California Institute of Technology, Pasadena, California, USA.
[6]National Exposure Research Laboratory, Office of Research and Development, U.S. EPA, NASA Langley Research Center, Hampton, Virginia, USA.
[7]National Institute of Aerospace, Hampton, Virginia, USA.
[8]Chemical Sciences Division, Earth Systems Research Laboratory, NOAA, Boulder, Colorado, USA.
[9]Department of Meteorology, Pennsylvania State University, University Park, Pennsylvania, USA.
[10]Laboratory for Atmospheres, NASA Goddard Space Flight Center, Greenbelt, Maryland, USA.
[11]Department of Physics and Astronomy, Valparaiso University, Valparaiso, Indiana, USA.

0148-0227/09/2008JD011337$09.00

exist when elevated background ozone and aerosol from distant regions affect Texas? (3) How high are background concentrations of ozone and aerosol, and how do they vary spatially and temporally? (4) Which areas within Texas adversely affect the air quality of nonattainment areas within Texas? (5) Which areas outside of Texas adversely affect the air quality of nonattainment areas within Texas?

[3] The current study addresses the latter two of these questions by quantifying the contributions of background (continental scale) ozone production on Houston and Dallas air quality during TexAQS II. To quantify background contributions we use ensemble Lagrangian trajectories, initialized at U.S. EPA AIRNow (http://www.airnow.gov/) monitoring sites within the Houston and Dallas metropolitan statistical areas (MSA), to identify remote source regions that impact Houston and Dallas background ozone distributions. Global-scale chemical analyses, constrained with composition measurements from instruments on the NASA Aura Satellite [*Schoeberl et al.*, 2006] are used to provide estimates of background composition along ensemble back trajectories. Comparison between the chemical analyses, airborne, balloon, and satellite data collected during the study period are used to verify the analyses used in the study. Lagrangian averaged O_3 net photochemical production (production minus loss, P-L) rates along the back trajectories are used as a metric to classify back trajectories.

2. RAQMS Modeling System

[4] The chemical modeling/assimilation tool used in this study is Real-time Air Quality Modeling System (RAQMS) [*Pierce et al.*, 2007]. RAQMS is a unified (stratosphere-troposphere) online global chemical and aerosol assimilation/forecasting system that has been used to support airborne field missions [*Pierce et al.*, 2003, 2007], develop capabilities for assimilating satellite trace gas retrievals [*Fishman et al.*, 2008] and assess the impact of global chemical analyses on regional air quality predictions [*Tang et al.*, 2007; *Song et al.*, 2008]. RAQMS analyses were conducted at 2×2 degrees horizontal resolution with 35 hybrid eta (sigma-theta) levels extending from the surface to approximately 60 km. The stratospheric resolution is approximately 3 km with 14 purely isentropic levels extending from 380 K (which corresponds to the tropical tropopause) to 2350 K. RAQMS has 21 eta levels in the troposphere that transition from nearly isentropic in the upper troposphere to purely sigma at the surface. The standard O_x-HO_x-NO_x-ClO_x-BrO_x cycles governing the formation and destruction of odd oxygen, tropospheric NO_x-HO_x reactions, oxidation of CH_4 and CO are considered [*Pierce et al.*, 2003]. The nonmethane hydrocarbon (NMHC) chemical scheme is based on the Carbon Bond-IV mechanism (CB-IV) [*Gery et al.*, 1989] with adjustments by *Zaveri and Peters* [1999]. Additional extensions implemented in RAQMS include a four-product isoprene oxidation scheme and the semiexplicit treatment of propane. Climatological emissions include anthropogenic and natural sources and are based largely on 1×1 degree public databases available from GEIA/EDGAR with updates for Asian emissions from *Streets et al.* [2003] and additional biogenic CO sources as described by *Duncan and Bey* [2004]. RAQMS biomass burning emissions includes daily, ecosystem and severity based estimates based on Moderate Resolution Imaging Spectroradiometer (MODIS) Terra and Aqua fire detections [*Al-Saadi et al.*, 2008]. Aircraft and lightning NO_x emissions are also included. RAQMS uses the statistical digital filter (SDF) analysis system [*Stobie*, 2000; J. M. Stobie et al., The use of optimum interpolation at AFGWC, paper presented at 7th Conference on Numerical Weather Prediction, American Meteorological Society, Boston, Massachusetts, 1985] to perform an optimal interpolation (OI) based univariate assimilation of satellite-based trace gas observations. RAQMS meteorological forecasts are initialized from NOAA Global Forecasting System (GFS) analyses at 6-h intervals. For further details on the RAQMS chemical mechanism and assimilation system see *Pierce et al.* [2007].

[5] The RAQMS TexAQS II chemical analysis includes assimilation of cloud cleared Ozone Monitoring Instrument (OMI) total column ozone OMI-TOMS collection 2 retrievals [*Levelt et al.*, 2006a, 2006b] and Version 2 (V002) ozone and carbon monoxide retrievals from the Tropospheric Emission Spectrometer (TES) nadir global survey measurements [*Beer*, 2006]. The OMI column ozone assimilation uses only cloud cleared retrievals and accounts for the vertical variation in retrieval sensitivity by convolving the model first guess ozone profile with the zonal mean, time averaged sensitivity and the 3D monthly ozone profile climatology (a priori) used in the OMI-TOMS retrieval algorithm prior to computing a first guess ozone column. Level 2 (L2) OMI-TOMS ozone retrievals are assimilated at 6-h intervals by aggregating measurements within ±3 h of 0000, 0600, 1200, and 1800 UT. The resulting total column ozone analysis increment (observation−first guess, O-F) is used to adjust the RAQMS first guess ozone profile by applying a uniform percentage adjustment throughout the column. Comparisons between correlative airborne measurements and OMI-TOMS total column ozone retrievals show agreement to within less than 1.0% [*Kroon et al.*, 2008].

[6] The RAQMS TES O_3 and CO assimilation occurs at 1-h intervals and uses the averaging kernel (a measure of the vertical sensitivity of the retrieval) and a priori provided in the TES L2 data product. The TES a priori is based on monthly mean mixing ratios from the Model for OZone And Related chemical Tracers (MOZART) [*Brasseur et al.*, 1998] chemical transport model. Retrievals from daily TES global survey mode observations between 60°S and 60°N were assimilated owing to low sensitivity to lower tropospheric ozone in polar latitudes. O_3 and CO retrievals with a "master" quality flag (SpeciesRetrievalQuality) equal to one are considered to be of good quality [*Osterman et al.*, 2007] and are candidates for assimilation. Since the TES L2 quality flags have been developed primarily for tropospheric retrievals we restricted assimilation of TES CO to below the local tropopause while TES O_3 was assimilated when either the first guess or retrieved ozone mixing ratio was less then 1 ppmv. Because we apply the TES averaging kernel to the RAQMS first guess as part of the TES observation operator, the resulting analysis increment is relatively smooth in the vertical. Consequently, smaller-scale vertical features that are resolved in the RAQMS first guess are retained. Because

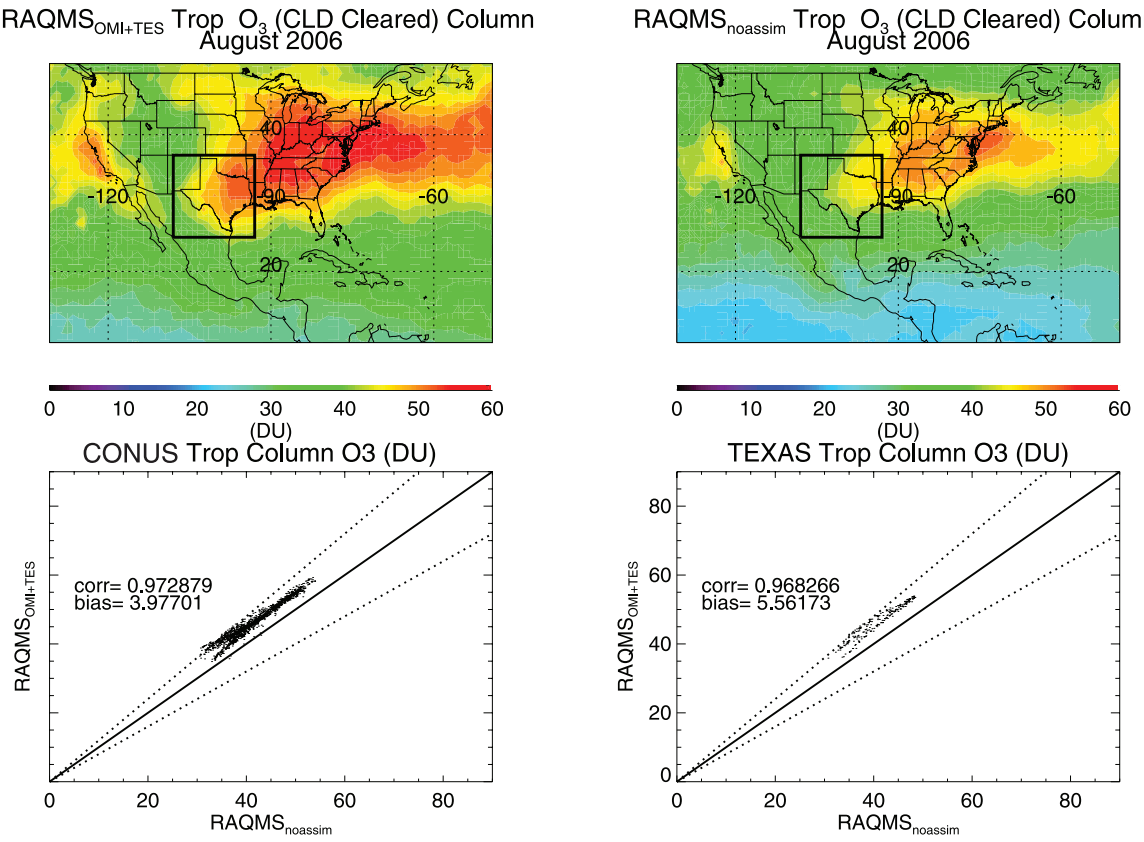

Figure 1. Comparison between RAQMS TES+OMI assimilation ($RAQMS_{TES+OMI}$) and RAQMS no-assimilation ($RAQMS_{noassim}$) tropospheric ozone columns (TOC) for August 2006. (top left) Mean $RAQMS_{TES+OMI}$ TOC (DU). (top right) Mean $RAQMS_{noassim}$ TOC (DU). Scatterplots of $RAQMS_{TES+OMI}$ versus $RAQMS_{noassim}$ over (bottom left) the continental United States and (bottom right) Texas along with correlation coefficients and mean biases. The continental United States (CONUS) scatterplots are for the entire region shown in the maps. The Texas scatterplots are for the region within the black box in the top panels. The solid line shows the 1-to-1 correlation, and the dashed line shows ±20% errors.

we include the TES a priori in the TES observation operator, the influence of the a priori in the retrieval is removed from the analysis increment. Under cloud free conditions, TES nadir ozone profiles have approximately four degrees of freedom giving an estimated vertical resolution of about 6 km in the troposphere [*Bowman et al.*, 2002, 2006; *Worden et al.*, 2004]. Comparison with correlative ozonesonde measurements during the period from October 2004 to October 2006 shows a 3–10 ppbv high bias in tropospheric ozone [*Nassar et al.*, 2008]. Agreement between TES and correlative airborne in situ CO profiles ranges from 10% to 35% in the lower and middle troposphere with TES being lower than the correlative measurements [*Luo et al.*, 2007].

[7] Estimates of the RAQMS forecast error variances for the assimilation scheme are calculated by inflating the analysis errors (a byproduct of the analysis) using the error growth model of *Savijarvi* [1995]. Constant observational errors of 10% of the global mean ozone column (OMI) and 10% of the globally averaged ozone on the RAQMS model levels (TES) are assumed. The quality control employed during the analysis includes three steps: (1) a gross check (which marks all observations that are obviously wrong based on threshold O-F values), (2) suspect identification (which marks observations that may be wrong based on O-F values), and (3) a buddy check (which involves performing the analysis without the gross or suspect observations and comparing the suspect O-F to the buddy check analysis increments).

[8] Figure 1 shows August monthly mean comparisons between the TES+OMI assimilation ($RAQMS_{TES+OMI}$) and no-assimilation ($RAQMS_{noassim}$) estimates of tropospheric ozone column (TOC) for August 2006. For these comparisons the RAQMS 6-h ozone analyses and forecasts were mapped to the L2 OMI total column ozone retrieval locations, and then the cloud-cleared assimilated and forecasted TOC was composited into 1 × 1 degree bins. OMI cloud reflectivity <15% was used for the cloud clearing. The analyzed and forecasted TOC both show a broad ozone maximum over the south central and eastern United States. However, the analyzed maximum is in excess of 50 DU while the forecasted maximum is near 45 DU. The analyzed TOC extends farther out over the western Atlantic than the forecasted TOC and shows a stronger localized ozone maximum off the California coast. Correlations between $RAQMS_{TES+OMI}$ and $RAQMS_{noassim}$ TOC are high over both the continental United States (CONUS) and Texas, with correlations of 0.972 and 0.968, respectively. On average, the TOC analysis is 3.9 DU higher than the

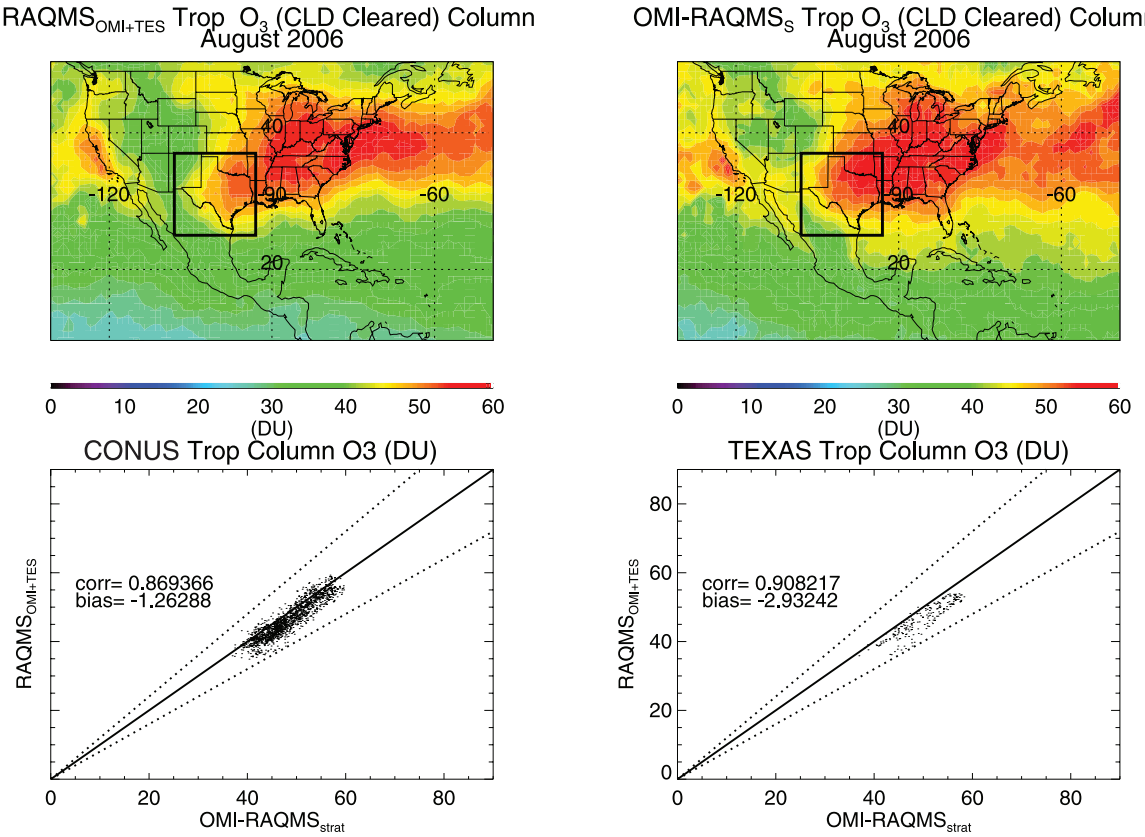

Figure 2. Comparison between RAQMS$_{TES+OMI}$ and OMI-RAQMS$_{strat}$ tropospheric ozone columns (TOC) for August 2006. (TOP LEFT) Mean RAQMS TOC (DU). (TOP RIGHT) Mean OMI-RAQMS$_{strat}$ TOC (DU). Scatterplots of RAQMS$_{TES+OMI}$ versus OMI-RAQMS$_{strat}$ over (bottom left) the continental United States and (bottom right) Texas along with correlation coefficients and mean biases. The continental United States (CONUS) scatterplots are for the entire region shown in the maps. The Texas scatterplots are for the region within the black box in the top panels. The solid line shows the 1-to-1 correlation, and the dashed line shows ±20% errors.

forecasted TOC over the continental United States and 5.5 DU higher over Texas during August 2006.

3. Verification of RAQMS Chemical Analysis

[9] Comparisons among RAQMS analyses, airborne, balloon and satellite data collected during the study period are used to verify the model analyses used in this study. We focus on validation of the analyzed O_3 and NO_2 since NO_x chemistry tends to dominate background ozone production [*McKeen et al.*, 1991]. Comparison with satellite trace gas measurements is used to characterize uncertainties in the continental-scale RAQMS analysis. Figure 2 shows August monthly mean comparisons between RAQMS$_{TES+OMI}$ and OMI based estimates of tropospheric ozone column (TOC) for August 2006. To estimate TOC from OMI total column ozone we subtract the stratospheric ozone column (from RAQMS 6-hourly analyses) from the cloud-cleared L2 OMI total column ozone retrieval (referred to as OMI-RAQMS$_{strat}$). For these comparisons the RAQMS 6-h ozone analyses were mapped to the L2 OMI total column ozone retrieval locations, the RAQMS stratospheric column was subtracted from the OMI total column, and then the cloud-cleared measured and modeled TOC was composited into 1 × 1 degree bins. The analyzed and observed TOC both show a broad ozone maximum in excess of 50 DU over the south central and eastern United States that extends out over the western Atlantic and a localized ozone maximum off the California coast. The RAQMS TOC analysis tends to underestimate the westward extent of the TOC enhancements relative to OMI-RAQMS$_{strat}$ and shows somewhat narrower meridional extent of the TOC enhancements over the western Atlantic. Correlations between RAQMS and OMI-RAQMS$_{strat}$ TOC are high over both the continental United States (CONUS) and Texas, with correlations of 0.869 and 0.908, respectively. The RAQMS TOC analysis shows a slight (−1.26 DU) low bias over the continental United States and a somewhat larger (−2.9 DU) bias over Texas during August 2006. Comparison of Figures 1 and 2 shows that the assimilation of OMI total column ozone and TES ozone profile retrievals results in significantly better estimates of the large-scale distribution of tropospheric ozone over the continental United States and Texas relative to OMI-RAQMS$_{strat}$ by reducing low biases in the RAQMS forecasted TOC.

[10] Figure 3 shows comparisons between RAQMS and OMI tropospheric NO_2 retrievals [*Bucsela et al.*, 2006] for August 2006. For these comparisons the RAQMS 6-h NO_2

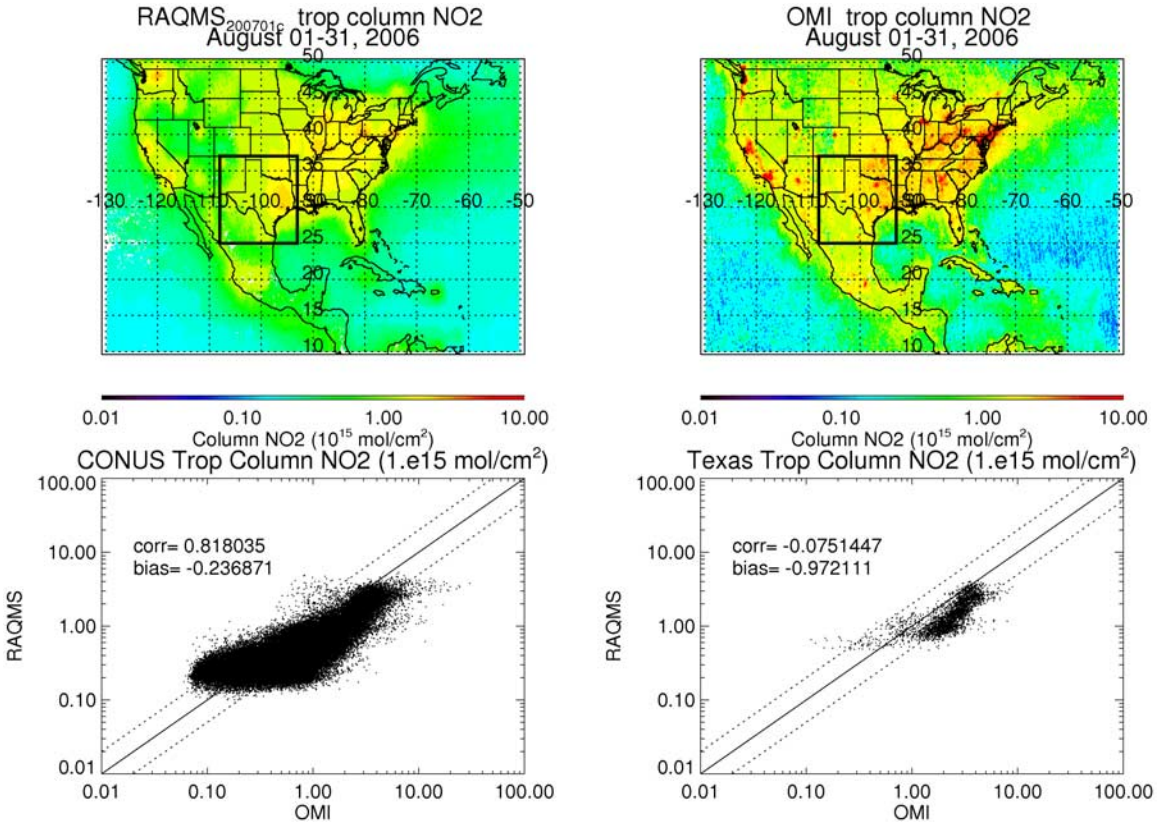

Figure 3. Comparison between RAQMS and OMI tropospheric NO_2 for August 2006. (top left) Mean RAQMS tropospheric NO_2 (10^{15} mol/cm^2). (top right) Mean OMI RAQMS tropospheric NO_2 (10^{15} mol/cm^2). Scatterplots of RAQMS versus OMI NO_2 over (bottom left) the continental United States and (bottom right) Texas along with correlation coefficients and mean biases. The continental United States (CONUS) scatterplots are for the entire region shown in the maps. The Texas scatterplots are for the region within the black box in the top panels. The solid line shows the 1-to-1 correlation, and the dashed line shows ± factor of 2 errors.

analyses were mapped to the L2 OMI tropospheric NO_2 retrieval locations and then the cloud-cleared measured and modeled tropospheric NO_2 were composited into 1×1 degree bins. The relatively coarse horizontal resolution of the RAQMS analysis does not capture the strong localized signatures of individual urban centers that are observed by OMI. However, on a continental scale the correlation between RAQMS and OMI tropospheric NO_2 is relatively high (0.81) because the regional-scale urban (Los Angeles, Oakland, Chicago, northeast corridor) and industrial (Ohio and Upper Mississippi River valleys) sources are resolved. Background RAQMS NO_2 is generally within a factor of 2 of the observed tropospheric NO_2 although RAQMS shows systematically lower background levels over the eastern and central United States and higher background levels over the central Atlantic and eastern Pacific, resulting of continental-scale mean biases of -0.23×10^{15} mol/cm^2. Background tropospheric NO_2 levels over eastern Texas are reasonably well represented with mean biases over Texas of -0.97223×10^{15} mol/cm^2 or 25–50%. However, the correlation between RAQMS and OMI tropospheric NO_2 is very poor over Texas because RAQMS does not resolve local maxima associated with Dallas, Houston, Austin, and Del Rio and overestimates background NO_2 over the Gulf of Mexico.

[11] Figure 4 shows comparisons between RAQMS and NOAA P3 in situ measurements of O_3 and NO_2 [*Ryerson et al.*, 2003] within east Texas during TexAQS II. For these comparisons the RAQMS 6-h O_3 and NO_2 analyses were mapped onto the 1-s P3 O_3 and NO_2 measurements for all TexAQS II flights (11 September to 13 October 2006) and then statistics (median, 50th, 90th percentile) where computed in 50 mbar pressure bins. The majority of the P3 flights were within the Houston MSA. RAQMS median NO_2 is up to 20% higher than observed within the Houston boundary layer (below 850 mbar) and in good agreement in the free troposphere resulting in an 18% overestimate in the median NO_2 column (obtained by integrating the median NO_2 profile between the surface and 650 mbar). The P3 shows significantly larger variability within the Houston boundary layer. The observed boundary layer NO_2 distribution is highly skewed toward large NO_2 mixing ratios (note the asymmetry in the 50th and 90th percentile) which would lead to higher mean mixing ratios and is consistent with the RAQMS underestimate of the mean Houston NO_2 column relative to OMI. The analyzed ozone is systematically high by 10 ppbv (~15%) throughout the column relative to the P3. Note that the mean ozone measured by the P3 is similar to that for the Houston ozonesondes [*Thompson et al.*, 2008, Figure 5d].

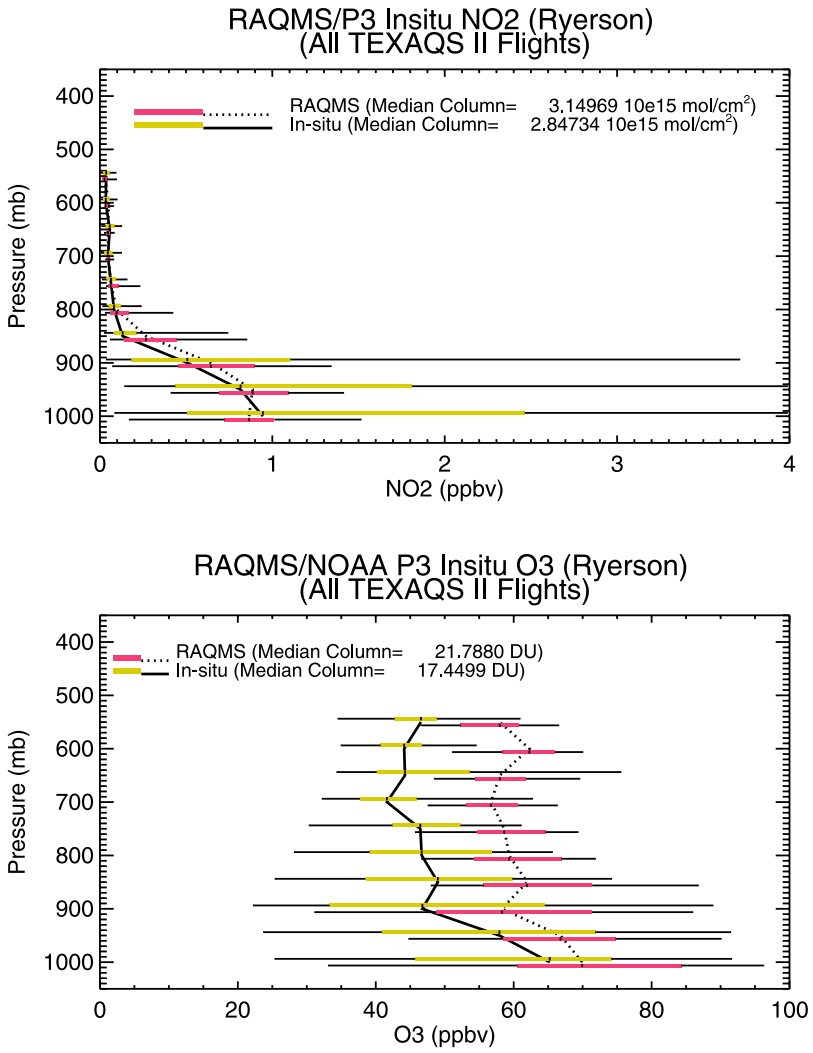

Figure 4. Comparison between RAQMS and NOAA P3 in situ (top) NO_2 and (bottom) O_3 for all flights during TexAQS II. Median mixing ratios (ppbv) are indicated by solid (observed) and dashed (RAQMS) lines. The 50th percentile (red and yellow bars) and 90th percentile (lines) within 50-mbar pressure intervals are also shown. The mean P3 profile is consistent with the mean of August 2006 ozonesonde profiles from midday daily launches over Houston [*Thompson et al.*, 2008].

This is in contrast to the underestimate in TOC relative to OMI-RAQMS$_{strat}$.

[12] Observation System Experiment (OSE) studies were conducted to further quantify the impact of TES and TES+OMI assimilation on the RAQMS ozone analysis. As part of IONS-06 [*Thompson et al.*, 2008] 376 North American ozonesondes were launched during August 2006, 19 of them at the University of Houston (29.7°N, 95.4°W). A series from 31 July to 11 September 2006, was launched from the Research Vessel *Ronald H. Brown* operating in the Houston-Galveston area. The full set of IONS-06 August sondes (373 sondes) is used to evaluate RAQMS O_3 with no assimilation, TES assimilation, and combined TES+OMI assimilation. RAQMS 6-hourly ozone profiles where horizontally and temporally interpolated to the ozonesonde measurement location and time and then vertically interpolated onto the full resolution sonde pressure levels. Mean percentage biases were computed over seven different pressure ranges to characterize the agreement between the RAQMS and IONS ozonesondes throughout the troposphere and stratosphere. The seven pressure ranges span the column(1000mb to 10mb), stratosphere (100 mbar to 10 mbar), middle stratosphere (50 mbar to 10 mbar), lower stratosphere (100 mbar to 50 mbar), troposphere (1000 mbar to 100 mbar), upper troposphere (300 mbar to 100 mbar), and lower troposphere (1000 mbar to 300 mbar), respectively. Results from this study are summarized in Table 1. With no ozone assimilation RAQMS systematically underestimates the overall column by −8.47% with tropospheric and stratosphere biases of −5.05% and −12.87%, respectively. The largest biases occur in the middle stratosphere (−17.63%). Lower tropospheric biases are −6.44% without assimilation. Assimilation of TES ozone profiles leads to reductions in overall column biases (−3.46%), and introduces a slight (3.32%) positive bias in the troposphere. TES assimilation does not significantly affect the stratosphere owing to the <1 ppmv threshold used in the assimilation. The TES results are consistent with results of

Table 1. Results of OSE Studies of the Impact of TES and Combined TES+OMI Ozone Assimilation on the RAQMS Chemical Analysis[a]

	No Assimilation	TES Assimilation	TES+OMI Assimilation
Column bias (%)	−8.47	−3.46	+0.30
Stratospheric bias (%)	−12.87	−12.17	+0.06
Middle stratosphere bias (%)	−17.63	−17.60	−5.18
Lower stratosphere bias (%)	−4.31	−2.40	+9.51
Tropospheric bias (%)	−5.05	+3.32	+0.49
Upper troposphere bias (%)	−3.65	+2.21	−11.31
Lower troposphere bias (%)	−6.44	+4.42	+12.29

[a]Biases are determined with respect to August 2006 IONS ozonesonde data. [*Thompson et al.*, 2007, 2008], consisting of more than 370 profiles during TexAQS-II. The accuracy of the sondes in the troposphere is ∼5–7% [*Smit et al.*, 2007].

GEOS-CHEM assimilation of TES retrievals [*Parrington et al.*, 2008] which show that assimilation of TES increases tropospheric ozone. The TES+OMI assimilation results in significant reductions in column, tropospheric, and stratospheric biases (all less then 1%), demonstrating the strong constraint that assimilation of OMI cloud-cleared total column ozone has on the RAQMS analysis. The combined TES+OMI assimilation leads to reductions in the middle stratospheric biases (−5.18%) but introduces relatively large lower stratospheric high biases (9.51%) which compensate each other, resulting in very small stratospheric biases. Similarly, the small tropospheric bias is the result of compensation between relatively large upper tropospheric low biases (−11.31%) and lower tropospheric high biases (12.29%). This lower tropospheric high bias is consistent with the ∼15% median bias relative to the P3 in situ measurements.

[13] The satellite and airborne based verification of the RAQMS O_3 and NO_2 analyses indicates that RAQMS is suitable for assessment of the influences of background NOx on O_3 production over the continental United States. However, the combined assimilation of TES+OMI introduces high biases in the lower troposphere. In addition, owing to the relatively coarse horizontal and vertical resolution of the RAQMS analysis, urban NO_2 mixing ratios are likely to be underestimated. DOAS measurements of NO_2 abundances within the Houston nocturnal boundary layer show gradients of 20–40 ppbv between the 20–70 m and 130–300 m intervals (J. Stutz, personal communication, October 2008) which cannot be resolved in the RAQMS analysis owing to the ∼60-m height of the lowest model layer. The inability to resolve high surface NO_2 abundances leads to underestimates in nighttime O_3 titration within the RAQMS model which subsequently leads to overestimates in daytime ozone within urban areas. These two factors necessitate the use of bias corrections for direct comparisons with AIRNow surface ozone measurements.

[14] The RAQMS analysis shows mean nighttime (0600 UT or 0100 local time (LT)) biases of 29.39 ppbv and mean daytime (1800 UT or 1300 LT) biases of 25.21 ppbv relative to the 33 AIRNow sites within the Houston MSA. We attribute this large overestimate in surface ozone within the Houston MSA to underestimates in nighttime titration of ozone under high urban NO_x environments. The RAQMS analyses shows mean nighttime biases of 16.39 ppbv and mean daytime biases of 18.41 ppbv relative to the 13 AIRNow sites within the Dallas MSA. We attribute this smaller overestimate in surface ozone within the Dallas MSA to less nocturnal titration of surface ozone. The role of nocturnal ozone titration in determining the high biases relative to urban AIRNow measurements is further supported by investigation of the Clarksville, Texas, AIRNow (site id 483870648, CAMS 648) which is a rural site located in northeast Texas near the Oklahoma border (95.06°E, 33.62°N). The Clarksville site is only occasionally influenced by urban emissions with only five titration events (nighttime ozone is less than 10 ppbv) during August–September 2006. The RAQMS analyses shows mean nighttime biases of 12.78 ppbv and mean daytime biases of 13.96 ppbv at Clarksville, Texas. These biases are in good agreement to the overall 12–15% high bias in the RAQMS analysis that was found in comparisons to the P3 and lower tropospheric IONS-06 ozonesonde measurements, which we attribute to assimilation of TES+OMI ozone retrievals.

4. Results

[15] *Darby* [2005] examined the impact of local wind patterns on surface ozone within the Houston metropolitan area during the 2000 TexAQS campaign and found that high-ozone days typically occurred during periods where the local (onshore) gulf breeze and large-scale (offshore) synoptic flow lead to small-scale convergence zones within the Houston area. These sea-breeze-induced convergence zones result in a band of weak or stagnate winds and occur when afternoon southeasterly to southerly sea breeze followed early morning weak northwesterly offshore synoptic flow. The east-west orientation of the sea-breeze convergence zone results in a buildup of ozone precursors over parts of Houston, leading to rapid ozone production (up to 140 ppbv/h) [*Daum et al.*, 2004].

[16] The synoptic situation that contributes to the Houston high-ozone events (weak offshore flow) often occurs in association with weak cold fronts which pass over east Texas and become stationary just offshore in the Gulf of Mexico. The synoptic circulation associated with these "trailing cold fronts" can lead to synoptic-scale convergence, accumulation of ozone precursors, and sustained ozone production during continental-scale transport. *Rappengluck et al.* [2008] examined synoptic flow patterns and surface ozone levels during August–September 2006 and found that Houston experienced high background surface ozone under postfrontal northerly or easterly transport of dry continental air at 850 hPa. Analysis of Houston ozonesonde data during 2006 [*Morris et al.*, 2009] shows that background ozone

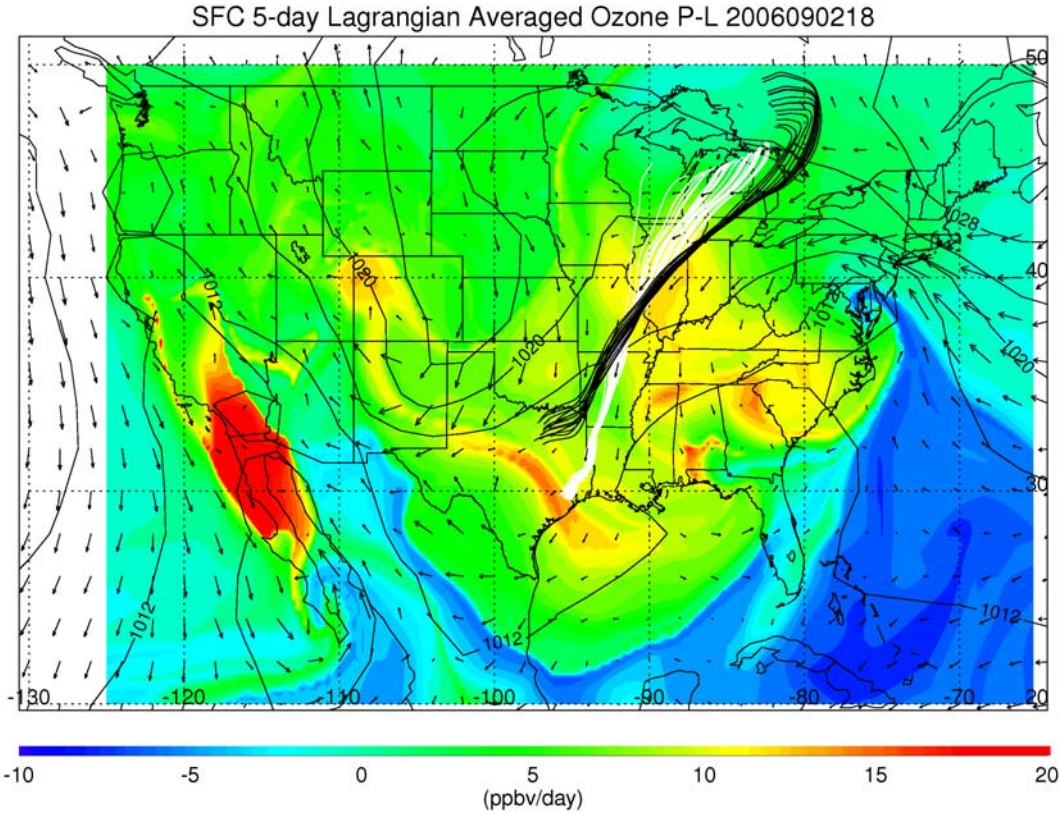

Figure 5. Synoptic distribution of 5-day Lagrangian averaged O_3 P-L (ppbv/d colored) for parcels initialized at the surface at 1300 LT on 2 September 2006. Five-day Houston (white) and Dallas (black) AIRNow ensemble back trajectories initialized at 1300 LT on 2 September 2006 and surface wind vectors and sea level pressure (mbar) are also shown.

levels ranged from 30 ppbv (marine) to nearly 60–70 ppbv (continental) throughout the lower troposphere. The current analysis extends these studies by using the RAQMS chemical analysis and ensemble Lagrangian trajectory techniques to characterize the amount of ozone production that occurs during synoptic-scale transport prior to arrival in the Houston and Dallas MSAs.

[17] Figure 5 provides an example of sustained background ozone production associated with a weak cold front that impacted ozone the Houston MSA on 2 September 2006. A map of Lagrangian averaged ozone production-loss (P-L) over the previous 5 days valid at 1300 LT on 2 September 2006 is obtained using Reverse Domain Filling (RDF) techniques [*Sutton et al.*, 1994]. To construct the map, a uniform ($0.25^\circ \times 0.25^\circ$) grid of trajectories is initialized at the lowest model level (~60 m) at 1300 LT on 2 September and the LaRC trajectory model [*Pierce and Fairlie*, 1993] is used to predict 5-day back trajectories. RAQMS 6-hourly averaged ozone P-L predictions are then averaged along each trajectory and the resulting Lagrangian mean O_3 P-L is then mapped back onto the original uniform grid. A region of high Lagrangian averaged O_3 P-L (>15 ppbv/d) extends across Texas from the Louisiana Gulf Coast toward New Mexico and is associated with north-northwesterly surface winds behind a surface low-pressure system that was centered over Virginia on 2 September. Lagrangian averaged O_3 P-L of 15 ppbv/d could potentially increase background ozone by 75 ppbv during transport to Houston. However, much of this in situ production is offset by depositional losses and turbulent boundary layer mixing processes as the air mass is transported from the upper Midwest to Houston. Five-day ensemble back trajectories, initialized at the locations of Houston and Dallas U.S. EPA AIRNow sites, are also shown in Figure 5. These ensemble AIRNow back trajectories serve as the basis for our estimates of the impact of background ozone on Houston and Dallas ozone. The Houston ensemble back trajectories show that the air mass with high Lagrangian averaged O_3 P-L had its origins in the upper Midwest, passed over Chicago, and was then advected southward along the lower Mississippi River valley prior to arrival in Houston. The Dallas ensemble back trajectories originated farther to the northeast in Ontario, passed to the south of Chicago, and moved into Dallas along the lower Mississippi River Valley.

[18] Figure 6 shows time series of the Lagrangian chemical evolution of ensemble back trajectories initialized from the Houston AIRNow sites at 1300 LT on 2 September 2006. Initial (−120 h) ensemble mean ozone mixing ratios are near 40–45 ppbv and reach 85 ppbv by the time they arrive in Houston. All of the Houston trajectories remain within the continental boundary layer which shows large diurnal growth along the 5-day back trajectories. Ensemble mean O_3 P-L reaches up to 30–40 ppbv/d in conjunction with increases in NO_y of up to 50 ppbv/d at −80 h (day 4). The largest Lagrangian NO_y P-L occurs at night owing to buildup of local NO_2 emissions within the shallow nocturnal boundary layer. The Houston ozonesonde structure in the lower troposphere during the preceding two days (31 August

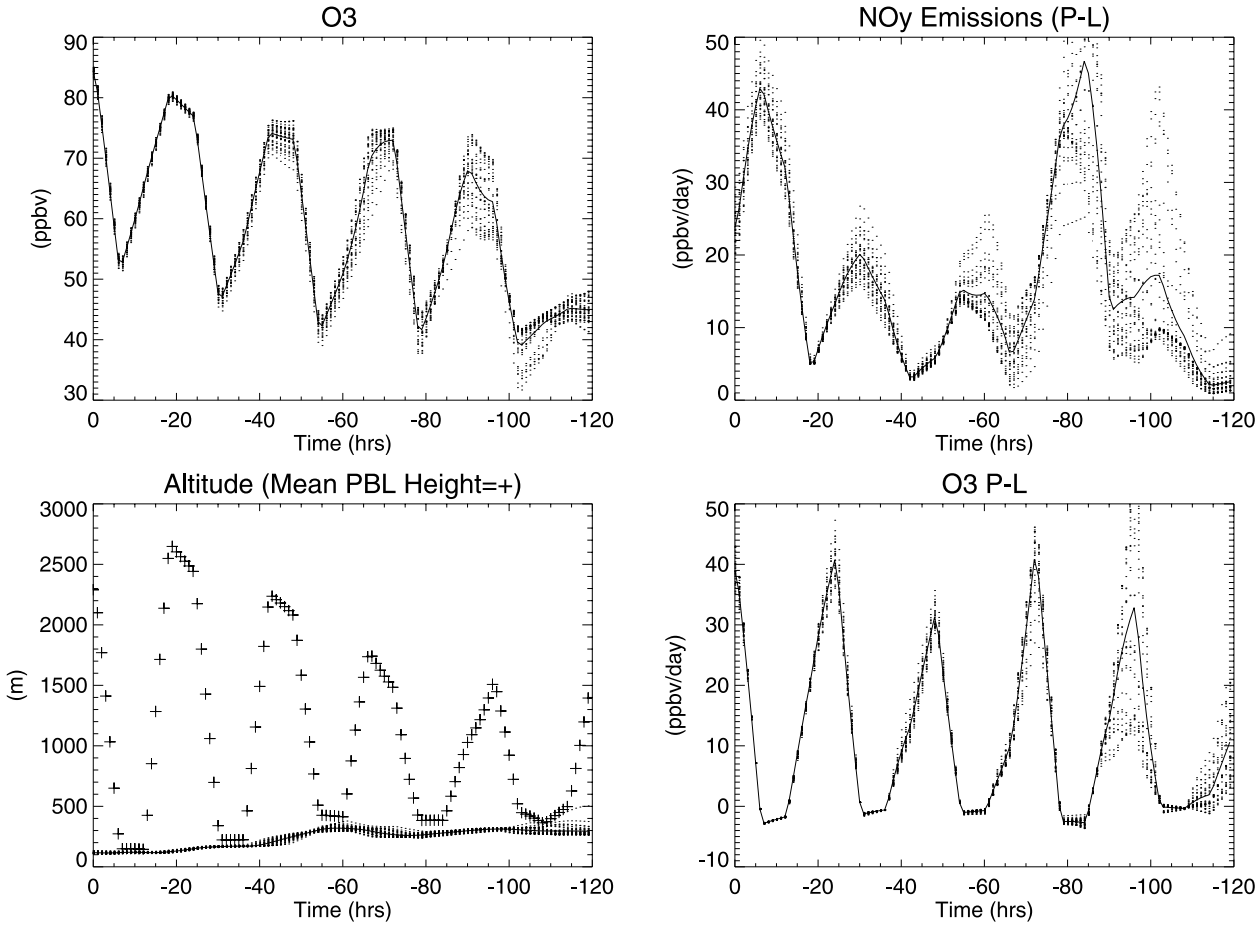

Figure 6. Lagrangian time series of ensemble chemical evolution for AIRNow surface back trajectories initialized at 1300 LT on 2 September 2006. (top left) Ensemble O_3 (ppbv), (top right) NO_y emissions (ppbv/d), (bottom left) altitude (meters), and (bottom right) O_3 P-L (ppbv/d) versus time (hours). The dots are the individual ensemble members and the solid line is the ensemble mean. Plus signs in the plot of ensemble altitude indicate the ensemble mean location of the top of the boundary layer.

and 1 September in Figure 5b of *Thompson et al.* [2008]), shows mixing within the boundary layer up to 1.7 km. One can use the sonde concentrations within the BL to estimate an ozone increase of ~35 ppbv/d during this period, consistent with our Lagrangian analyses.

[19] To quantify the contributions of background ozone production within the Houston and Dallas MSAs we used daily 1300 LT ensemble back trajectories initialized from the U.S. EPA AIRNow sites within each MSA (as illustrated for 2 September in Figures 5 and 6) to sample the RAQMS chemical analysis during the period from 15 July through 15 October 2006. Daily "Background" O_3 mixing ratios were determined by ensemble averaging the Houston and Dallas back trajectories just prior to arrival within the respective MSA (defined using a 2° radius about Dallas and Houston). The 2° radius was chosen since it fully encloses the region of strong urban emissions for both Houston and Dallas and does not result in any overlap between the Houston and Dallas MSAs. Daily "MSA" O_3 mixing ratios were determined by averaging the predicted O_3 at the Houston and Dallas AIRNow sites. Lagrangian averaged O_3 P-L rates along the back trajectories were used as a metric to classify back trajectories. The Lagrangian averages were computed during time periods when the back trajectories were outside the respective MSA. Three trajectory classes were considered based on ensemble mean ozone production (EM P-L): (1) enhanced background ozone production (EM P-L > 10 ppbv/d), (2) moderate background ozone production (0 < EM P-L < 10 ppbv/d), and (3) background ozone destruction (EM P-L < 0 ppbv/d).

[20] Ensemble back trajectories were computed for 33 U.S. EPA AIRNow sites in the Houston MSA. A time series depiction of the RAQMS back trajectory analysis of background influences on Houston O_3 is shown in Figure 7. The red line shows the observed Houston MSA mean and standard deviations of the 1300 LT AIRNow surface measurements. Periods with MSA mean ozone above 60ppbv (considered high-ozone days in this analysis) are indicted by asterisks. The blue lines show ensemble means from the RAQMS back trajectories. The solid blue is the predicted MSA mean (at Houston AIRNow sites) and the dashed blue is the predicted background mean. Both of the RAQMS time series were bias corrected using a constant correction of −25.2 ppbv to adjust for RAQMS overestimates in surface ozone relative to the Houston AIRNow sites. The RAQMS MSA mean does a good job of tracking the observed daily variations in Houston surface ozone although the RAQMS analysis underestimates peak MSA

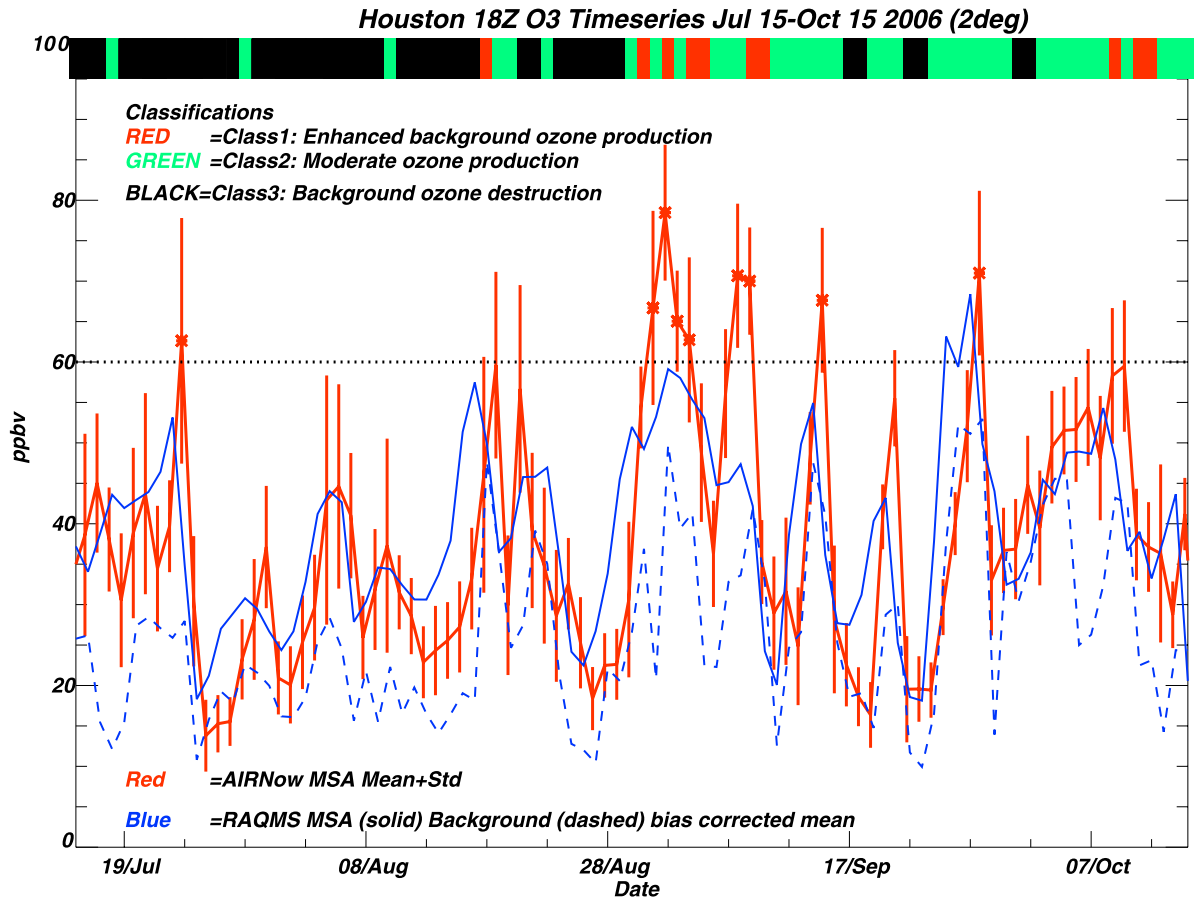

Figure 7. Time series of Houston AIRNow MSA (red line), bias-corrected RAQMS MSA (solid blue line), and bias-corrected RAQMS background (dashed blue line) ensemble mean ozone (ppbv) during the period from 15 July (Julian day 196) to 15 October (Julian day 288) 2006. The colored bar at the top indicates the air mass classification based on the ensemble mean background O_3 P-L (enhanced, moderate, or destruction) on each day.

mean ozone during the high-ozone events. The RAQMS background mean shows that in general, periods of high ozone within the Houston MSA are associated with high background ozone along the ensemble Houston back trajectories. The difference between the RAQMS MSA and background mean time series indicates the amount of ozone produced within the Houston MSA according to RAQMS. During periods when Houston experiences low to moderate ozone, such as 24 July to 28 August and 27 September to 15 October, the bias-corrected RAQMS MSA mean is in good agreement with the observed MSA mean. During periods when Houston experiences high ozone (indicated by asterisks), the bias-corrected RAQMS MSA mean tends to be underestimated. The color bar along the upper part of the time series indicates the background influence classification based on the ensemble mean ozone production on each day. During the first half of the TexAQS II analysis period (prior to 28 August), Houston inflow was dominated by background ozone destruction (Class 3) with only 1 day with observed MSA mean ozone greater than 60 ppbv. During the second half of the TexAQS II analysis period (28 August), Houston inflow was dominated by moderate to enhanced background ozone production (Classes 1 and 2). Enhanced regional ozone production influenced the Houston MSA on 10% of the days during 15 July to 15 October 2006 TexAQS II period. However, the Lagrangian analysis shows that enhanced background O_3 production as associated with six out of nine periods with high O_3 within the Houston MSA during the study period.

[21] Periods when background ozone destruction (Class 3) influences the Houston MSA occurred on 48% of the days during the study period and are associated with synoptic-scale onshore flow from the Gulf of Mexico. Periods when moderate or enhanced background ozone production influences Houston MSA occurred on 42% of the days during the study period and are associated with synoptic-scale flow patterns that bring continental air masses into the Houston MSA. Maps of mean RAQMS O_3 P-L and NOy source strengths for days when enhanced background O_3 production (Class 1) impacted the Houston MSA are shown in Figure 8. These maps were constructed by binning hourly estimates of O_3 P-L and NO_y P-L along the Class 1 trajectories in $2^\circ \times 2^\circ$ latitude and longitude bins during the period from 10 July through 15 October 2006. Houston enhanced regional O_3 production events have a Midwest/Ohio River Valley source with significant O_3 P-L (40 ppbv/d) due to high NO_x sources (30 ppbv/d) along the southern Great Lakes. Houston also contributes to enhanced background O_3 production events owing to recirculation of Houston emissions.

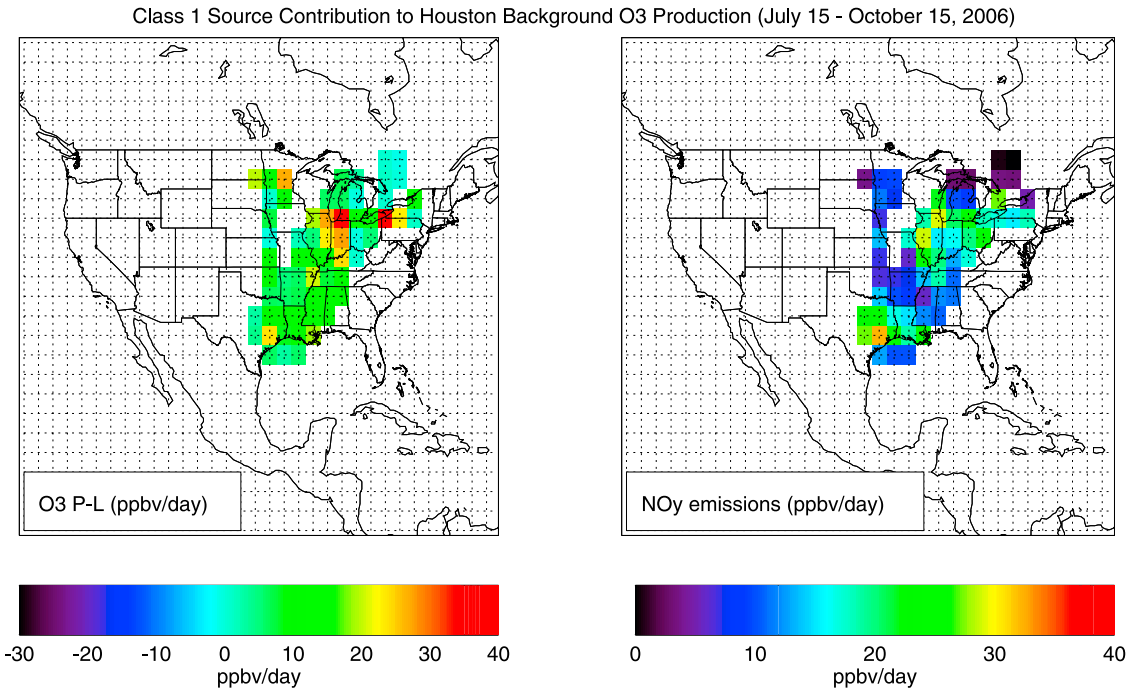

Figure 8. Map of source contributions for Houston Class 1 (background P-L > 10ppbv/d) days. (left) Mean O_3 P-L (ppbv/d) and (right) NO_y emissions (ppbv/d) are colored.

[22] Ensemble back trajectories were run for 13 U.S. EPA AIRNow sites in the Dallas MSA. Figure 9 shows the Lagrangian time series analysis of background influences for Dallas. The RAQMS ensemble mean MSA and background ozone time series have been adjusted by −18.4 ppbv to account for the high bias relative to the Dallas AIRNow measurements. The bias-corrected RAQMS prediction of Dallas MSA ensemble mean O_3 tracks the evolution of the observations quite well, although again, periods with high ozone tend to be underestimated. Dallas is less influenced by periods of background ozone destruction then Houston, with only 28% of the days during the study period showing ensemble mean ozone destruction. Instead, periods of moderate background ozone production dominate the Dallas inflow, accounting for 60% of the days during the study period. Enhanced regional ozone production influenced the Dallas MSA on the remaining 12% of the days during the study period. Overall, 7 out of 15 Dallas periods with elevated O_3 (greater than 60 ppbv) were associated with enhanced background ozone production during the TexAQS II analysis period. Figure 10 shows the map of mean O_3 P-L and NO_y source strengths for days when enhanced background O_3 production impacted the Dallas MSA. On average, periods of enhanced background O_3 production events in Dallas have a broad Great Plains/Midwest/Ohio River Valley source with significant O_3 P-L (20–30 ppbv/d) due to Chicago and Houston NO_x sources which reach 40 ppbv/d and >30 ppbv/d, respectively.

5. Sensitivity Analysis

[23] The sensitivity of our results to the assumed 2° radius for determining "background" verses MSA O_3 mixing ratios was explored by considering a 4° radius for ensemble averaging the Houston and Dallas back trajectories prior to arrival within the respective MSA. Using a 4° radius results in a 40% reduction for Houston and a 30% reduction for Dallas in the number of days that are classified as periods with enhanced background O_3 production. The reduction in enhanced background ozone classifications results in two Houston high-ozone days (30 August and 8 September) and one Dallas high-ozone day (19 August) that are reclassified as moderate background ozone production using a 4° radius around the respective MSAs. Consequently, enhanced background O_3 production is associated with 4 out of 9 Houston periods and 6 out of 15 Dallas periods with elevated O_3 (greater than 60 ppbv) during the study period using a 4° radius. In addition, there are 3 days (18 July, 24 July, and 29 September) where the Houston back trajectories remain within 4° of Houston for the entire 5-day period.

[24] A 4° radius around Houston covers all of east Texas (including urban emissions from Dallas, Austin, Waco, and Brownsville) and most of Louisiana. Similarly, a 4° radius around Dallas covers most of east Texas (including urban emissions from Houston, Austin and Waco) and most of Oklahoma. Consequently, the enhanced background O_3 production classification using a 4° radius excludes intraregional transport events (i.e., effects of Houston emissions on Dallas). The sensitivity tests show that intraregional transport accounts for a significant fraction of the days with enhanced background ozone production for both Houston and Dallas.

6. Summary and Conclusions

[25] This study demonstrates how global chemical data assimilation systems, combined with Lagrangian trajectory techniques, can be used to quantify the impacts of back-

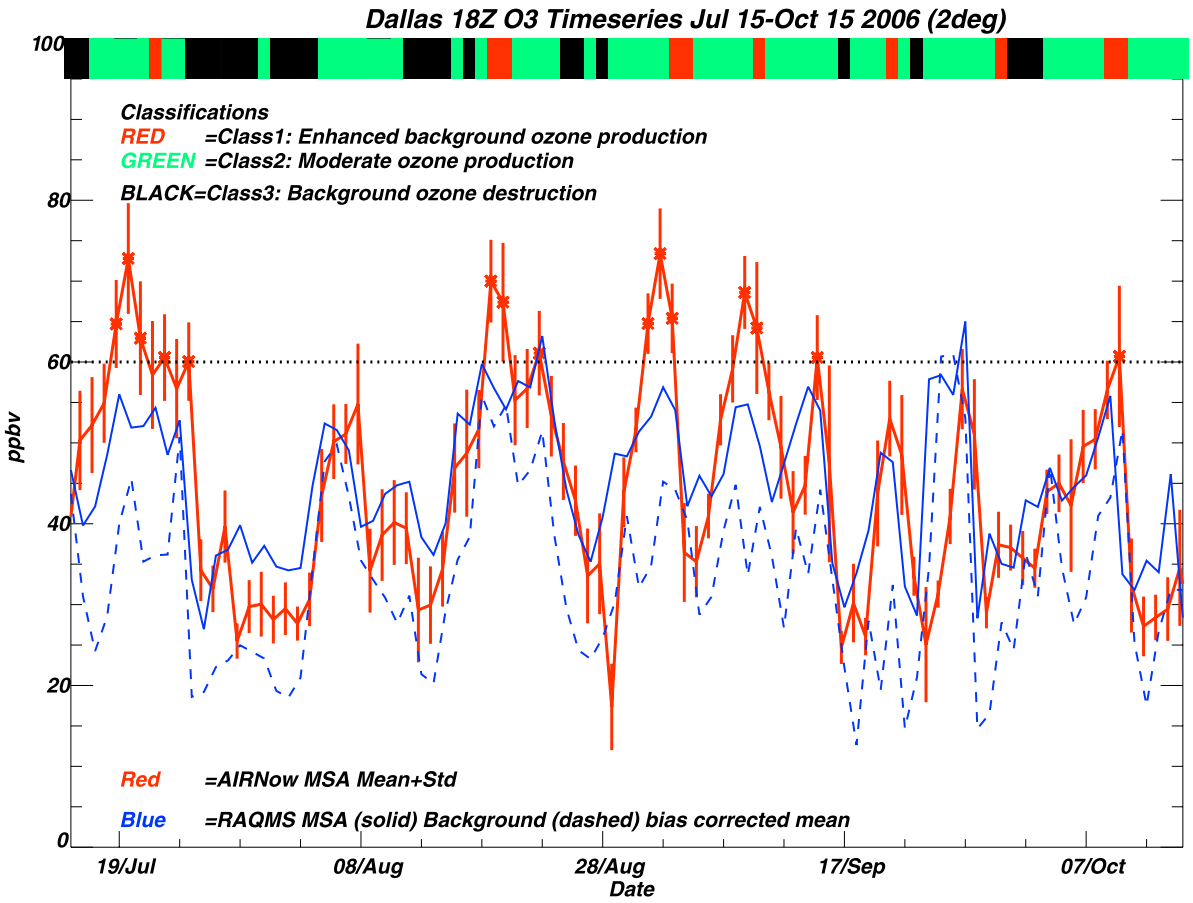

Figure 9. Same as Figure 7 for Dallas MSA.

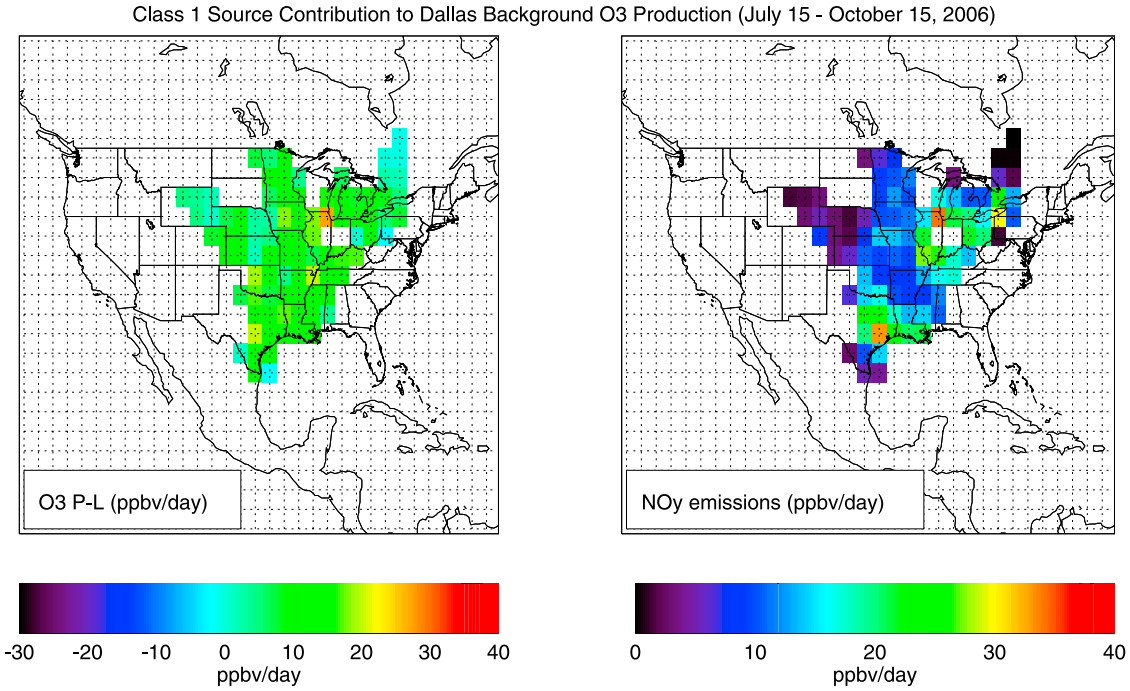

Figure 10. Same as Figure 8 for Dallas MSA.

ground ozone production on the Houston and Dallas metropolitan areas. Satellite based verification of the RAQMS chemical analysis, which shows that the observed continental-scale tropospheric ozone and NO_2 columns are well represented in the RAQMS analysis, provide confidence that RAQMS estimates of background ozone production are reasonable. Results of ensemble mean Lagrangian studies show that the majority (6 out of 9 or 66%) of the periods of high ozone in Houston were associated with periods of enhanced background ozone production. Source apportionment studies show that 5-day Lagrangian averaged O_3 P-L in excess of 15 ppbv/d can occur during continental-scale transport to Houston owing to NO_y enhancements from emissions within the southern Great Lakes as well as recirculation of the Houston emissions. Slightly less than 50% (7 out of 15) of the days with high ozone in the Dallas MSA show enhanced background ozone production associated with NO_y enhancements from emissions within Chicago and Houston. Sensitivity studies with a 4° versus 2° radius threshold for defining ''background'' conditions were conducted to examine the contributions from intraregional transport events. These sensitivity studies showed that 40% of the Houston and 30% of the Dallas periods with enhanced background ozone production were associated with east Texas intraregional transport events. If these events are excluded from the enhanced background ozone production classification then the ensemble Lagrangian studies show that 44% (4 out of 9) of the Houston and 40% (6 out of 15) of the Dallas days with high ozone show enhanced background ozone production associated with sources outside of east Texas during the study period.

[26] These results are broadly consistent with aircraft-based estimates of background ozone contributions during TexAQS II reported by *Kemball-Cook et al.* [2009]. They used upwind aircraft measurements to provide an estimate of background ozone concentrations and found that transported ozone contributed an average of 60 ppbv during the four Houston ozone exceedance days that were analyzed during 2006. However, direct comparisons with our estimates cannot be made, since the upwind aircraft measurements were still within the Houston and Dallas MSAs, whereas our background ozone estimates represent regional- to continental-scale inflow conditions that are 2° (~190 km) away from the Houston MSA. These results should also be interpreted in light of Houston and Dallas aircraft-based verification of the RAQMS chemical analysis which shows that while RAQMS captures the median profiles of NO_2 and O_3 over eastern Texas, at a horizontal resolution of 2×2 degrees RAQMS tends to significantly underestimate NO_2 variability, particularly at the high end of the observed NO_2, thereby underestimating rapid daytime ozone production and nighttime ozone titration within urban plumes. This underestimate of urban photochemistry not only impacts our estimates of local ozone production within Houston and Dallas but also our estimates of net O_3 P-L within the remote urban centers that are identified as source regions in the Lagrangian analysis. Continental-scale, high-resolution modeling studies should be conducted to address these issues.

[27] **Acknowledgments.** Thanks go to Bruce Doddridge of the National Aeronautics and Space Administration, Tropospheric Chemistry Program, and Fred Fehsenfeld of the National Oceanic and Atmospheric Administration Earth Systems Research Laboratory for coordinating the NASA involvement in the TexAQS II field mission. Thanks go to an anonymous reviewer for suggesting the sensitivity studies used to examine the role of intraregional transport during the Houston and Dallas high-ozone days. Support for IONS-06 and RAQMS came from the NASA Tropospheric Chemistry Program. The views, opinions, and findings contained in this report are those of the author(s) and should not be construed as an official National Oceanic and Atmospheric Administration or U.S. Government position, policy, or decision. This research used resources of the National Energy Research Scientific Computing Center, which is supported by the Office of Science of the U.S. Department of Energy under contract DE-AC02-05CH11231.

References

Al-Saadi, J. A., et al. (2008), Intercomparison of near-real-time biomass burning emissions estimates constrained by satellite fire data, *J. Appl. Remote Sens.*, *2*, 021504, doi:10.1117/1.2948785.

Beer, R. (2006), TES on the Aura mission: Scientific objectives, measurements, and analysis overview, *IEEE Trans. Geosci. Remote Sens.*, *44*, 1102–1105, doi:10.1109/TGRS.2005.863716.

Berkowitz, C. M., T. Jobson, G. Jiang, C. W. Spicer, and P. V. Doskey (2004), Chemical and meteorological characteristics associated with rapid increases of O_3 in Houston, Texas, *J. Geophys. Res.*, *109*, D10307, doi:10.1029/2003JD004141.

Bowman, K. W., T. Steck, H. M. Worden, J. Worden, S. Clough, and C. Rodgers (2002), Capturing time and vertical variability of tropospheric ozone: A study using TES nadir retrievals, *J. Geophys. Res.*, *107*(D23), 4723, doi:10.1029/2002JD002150.

Bowman, K. W., et al. (2006), Tropospheric Emission Spectrometer: Retrieval method and error analysis, *IEEE Trans. Geosci. Remote Sens.*, *44*, 1297–1307, doi:10.1109/TGRS.2006.871234.

Brasseur, G. P., D. A. Hauglustaine, S. Walters, R. J. Rasch, J.-F. Müller, C. Granier, and X. X. Tie (1998), MOZART: A global chemical transport model for ozone and related chemical tracers: 1. Model description, *J. Geophys. Res.*, *103*, 28,265–28,289, doi:10.1029/98JD02397.

Bucsela, E., E. Celarier, M. Wenig, J. Gleason, P. Veefkind, K. F. Boersma, and E. Brinksma (2006), Algorithm for NO_2 vertical column retrieval from the Ozone Monitoring Instrument, *IEEE Trans. Geosci. Remote Sens.*, *44*, 1245–1258, doi:10.1109/TGRS.2005.863715.

Darby, L. S. (2005), Cluster analysis of surface winds in Houston, Texas, and the impact of wind patterns on ozone, *J. Appl. Meteorol.*, *44*, 1788–1806.

Daum, P. H., L. I. Kleinman, S. R. Springston, L. J. Nunnermacker, Y.-N. Lee, J. Weinstein-Lloyd, J. Zheng, and C. M. Berkowitz (2004), Origin and properties of plumes of high ozone observed during the Texas 2000 Air Quality Study (TexAQS 2000), *J. Geophys. Res.*, *109*, D17306, doi:10.1029/2003JD004311.

Duncan, B. N., and I. Bey (2004), A modeling study of the export pathways of pollution from Europe: Seasonal and interannual variations (1987–1997), *J. Geophys. Res.*, *109*, D08301, doi:10.1029/2003JD004079.

Fishman, J., et al. (2008), Remote sensing of tropospheric pollution from space, *Bull. Am. Meteorol. Soc.*, *89*, 805–821, doi:10.1175/2008BAMS2526.1.

Gery, M. W., G. Z. Whitten, J. P. Killus, and M. C. Dodge (1989), A photochemical kinetics mechanism for urban and regional scale computer modeling, *J. Geophys. Res.*, *94*, 12,925–12,956, doi:10.1029/JD094iD10p12925.

Kemball-Cook, S., D. Parrish, T. Ryerson, U. Nopmongcol, J. Johnson, E. Tai, and G. Yarwood (2009), Contributions of regional transport and local sources to ozone exceedances in Houston and Dallas: Comparison of results from a photochemical grid model to aircraft and surface measurements, *J. Geophys. Res.*, *114*, D00F02, doi:10.1029/2008JD010248.

Kroon, M., I. Petropavlovskikh, R. Shetter, S. Hall, K. Ullmann, J. P. Veefkind, R. D. McPeters, E. V. Browell, and P. F. Levelt (2008), OMI total ozone column validation with Aura-AVE CAFS observations, *J. Geophys. Res.*, *113*, D15S13, doi:10.1029/2007JD008795.

Levelt, P. F., G. H. J. van den Oord, M. R. Dobber, A. Malkki, H. Visser, J. de Vries, P. Stammes, J. O. V. Lundell, and H. Saari (2006a), The Ozone Monitoring Instrument, *IEEE Trans. Geosci. Remote Sens.*, *44*, 1093–1101, doi:10.1109/TGRS.2006.872333.

Levelt, P. F., E. Hilsenrath, G. W. Leppelmeier, G. H. J. van den Oord, P. K. Bhartia, J. Tamminen, J. F. de Haan, and J. P. Veefkind (2006b), Science objectives of the Ozone Monitoring Instrument, *IEEE Trans. Geosci. Remote Sens.*, *44*, 1199–1208, doi:10.1109/TGRS.2006.872336.

Luo, M., et al. (2007), TES carbon monoxide validation with DACOM aircraft measurements during INTEX-B 2006, *J. Geophys. Res.*, *112*, D24S48, doi:10.1029/2007JD008803.

McKeen, S. A., et al. (1991), A study of the dependence of rural ozone on ozone precursors in the eastern United States, *J. Geophys. Res.*, *96*, 15,377–15,394, doi:10.1029/91JD01282.

Morris, G. A., B. Ford, A. Mefferd, B. Lefer, and B. Rappenglueck (2009), An evaluation of the influence of the morning residual layer on afternoon ozone concentrations in Houston using ozonesonde data, *Atmos. Environ.*, in press.

Nassar, R., et al. (2008), Validation of Tropospheric Emission Spectrometer (TES) nadir ozone profiles using ozonesonde measurements, *J. Geophys. Res.*, *113*, D15S17, doi:10.1029/2007JD008819.

Osterman, G. B., et al. (2007), Tropospheric Emission Spectrometer TES L2 data user's guide, version 3.00, 4 May 2007, technical report, Jet Propul. Lab., Calif. Inst. of Technol., Pasadena.

Parrington, M., D. B. A. Jones, K. W. Bowman, L. W. Horowitz, A. M. Thompson, D. Tarasick, and J. C. Witte (2008), Constraining the summertime tropospheric ozone distribution over North America through assimilation of observations from the Tropospheric Emission Spectrometer, *J. Geophys. Res.*, *113*, D18307, doi:10.1029/2007JD009341.

Pierce, R. B., and T. D. Fairlie (1993), Chaotic advection in the stratosphere: Implications for the dispersal of chemically perturbed air from the polar vortex, *J. Geophys. Res.*, *98*, 18,589–18,595, doi:10.1029/93JD01619.

Pierce, R. B., et al. (2003), Regional Air Quality Modeling System (RAQMS) predictions of the tropospheric ozone budget over east Asia, *J. Geophys. Res.*, *108*(D21), 8825, doi:10.1029/2002JD003176.

Pierce, R. B., et al. (2007), Chemical data assimilation estimates of continental U. S. ozone and nitrogen budgets during the Intercontinental Chemical Transport Experiment–North America, *J. Geophys. Res.*, *112*, D12S21, doi:10.1029/2006JD007722.

Rappengluck, B., R. Perna, S. Zhong, and G. A. Morris (2008), An analysis of the vertical structure of the atmosphere and the upper-level meteorology and their impact on surface ozone levels in Houston, Texas, *J. Geophys. Res.*, *113*, D17315, doi:10.1029/2007JD009745.

Ryerson, T. B., et al. (2003), Effect of petrochemical industrial emissions of reactive alkenes and NO_x on tropospheric ozone formation in Houston, Texas, *J. Geophys. Res.*, *108*(D8), 4249, doi:10.1029/2002JD003070.

Savijarvi, H. (1995), Error growth in a large numerical forecast system, *Mon. Weather Rev.*, *123*, 212–221.

Schoeberl, M. R., et al. (2006), Overview of the EOS-Aura mission, *IEEE Trans. Geosci. Remote Sens.*, *44*, 1066–1074, doi:10.1109/TGRS.2005.861950.

Smit, H. G. J., et al. (2007), Assessment of the performance of ECC-ozonesondes under quasi-flight conditions in the environmental simulation chamber: Insights from the Jülich Ozone Sonde Intercomparison Experiment (JOSIE), *J. Geophys. Res.*, *112*, D19306, doi:10.1029/2006JD007308.

Song, C.-K., D. W. Byun, R. B. Pierce, J. A. Alsaadi, T. K. Schaack, and F. Vukovich (2008), Downscale linkage of global model output for regional chemical transport modeling: Method and general performance, *J. Geophys. Res.*, *113*, D08308, doi:10.1029/2007JD008951.

Stobie, J. M. (2000), Algorithm theoretical basis document for statistical digital filter (SDF) analysis system (stretch-grid version), report, Data Assim. Off., NASA Goddard Space Flight Cent., Greenbelt, Md.

Streets, D. G., et al. (2003), An inventory of gaseous and primary aerosol emissions in Asia in the year 2000, *J. Geophys. Res.*, *108*(D21), 8809, doi:10.1029/2002JD003093.

Sutton, R. T., H. Maclean, R. Swinbank, A. O'Neill, and F. W. Taylor (1994), High resolution stratospheric tracer fields estimated from satellite observations using Lagrangian trajectory calculations, *J. Atmos. Sci.*, *51*, 2995–3005, doi:10.1175/1520-0469(1994)051<2995:HRSTFE>2.0.CO;2.

Tang, Y., et al. (2007), Influence of lateral and top boundary conditions on regional air quality prediction: A multiscale study coupling regional and global chemical transport models, *J. Geophys. Res.*, *112*, D10S18, doi:10.1029/2006JD007515.

Thompson, A. M., et al. (2007), Intercontinental Transport Ozonesonde Network Study (IONS, 2004): 1. Summertime upper troposphere/lower stratosphere ozone over northeastern North America, *J. Geophys. Res.*, *112*, D12S12, doi:10.1029/2006JD007441.

Thompson, A. M., J. E. Yorks, S. K. Miller, J. C. Witte, K. M. Dougherty, G. A. Morris, D. Baumgardner, L. Ladino, and B. Rappenglueck (2008), Tropospheric ozone sources and wave activity over Mexico City and Houston during Milagro/Intercontinental Transport Experiment (INTEX-B) Ozonesonde Network Study, 2006 (IONS-06), *Atmos. Chem. Phys.*, *8*, 5113–5126.

Worden, J. S., S. S. Kulawik, M. Shepard, S. Clough, H. Worden, K. Bowman, and A. Goldman (2004), Predicted errors of Tropospheric Emission Spectrometer nadir retrievals from spectral window selection, *J. Geophys. Res.*, *109*, D09308, doi:10.1029/2004JD004522.

Zaveri, R. A., and L. K. Peters (1999), A new lumped structure photochemical mechanism for large-scale applications, *J. Geophys. Res.*, *104*, 30,387–30,415, doi:10.1029/1999JD900876.

J. Al-Saadi and J. Szykman, Chemistry and Dynamics Branch, Science Directorate, NASA Langley Research Center, MS401B, Hampton, VA 23681, USA.

P. Bhartia, Laboratory for Atmospheres, Code 613, NASA Goddard Space Flight Center, Greenbelt, MD 20771, USA.

K. Bowman, Jet Propulsion Laboratory, California Institute of Technology, 4800 Oak Grove Drive, MS 183-601, Pasadena, CA 91109, USA.

C. Kittaka, Science Systems and Applications, Inc., Enterprise Parkway, Suite 200, Hampton, VA 23666, USA.

A. Lenzen and T. Schaack, Space Science and Engineering Center, University of Wisconsin, Madison, WI 53706, USA.

G. A. Morris, Department of Physics and Astronomy, Valparaiso University, 1610 Chapel Drive East, Valparaiso, IN 46383, USA.

R. B. Pierce, Center for Satellite Applications and Research, Cooperative Research Program, Advanced Satellite Products Branch, NESDIS, NOAA, 1225 West Dayton Street, Madison, WI 53706, USA. (brad.pierce@noaa.gov)

T. Ryerson, Chemical Sciences Division, Earth Systems Research Laboratory, NOAA, 325 Broadway, Boulder, CO 80305, USA.

A. Soja, National Institute of Aerospace, 100 Exploration Way, Hampton, VA 23666, USA.

A. M. Thompson, Department of Meteorology, Pennsylvania State University, University Park, PA 16802, USA.